CELL CYCLE
2017, VOL. 16, NO. 5, 406–414
http://dx.doi.org/10.1080/15384101.2016.1220461

Taylor & Francis
Taylor & Francis Group

REPORT

Cell-cycle-dependent drug-resistant quiescent cancer cells induce tumor angiogenesis after chemotherapy as visualized by real-time FUCCI imaging

Shuya Yano[a,b,c], Kiyoto Takehara[a,b,c], Hiroshi Tazawa[d], Hiroyuki Kishimoto[c], Yasuo Urata[e], Shunsuke Kagawa[c], Toshiyoshi Fujiwara[c], and Robert M. Hoffman[a,b]

[a]AntiCancer, Inc., San Diego, CA, USA; [b]Department of Surgery, University of California San Diego, CA, USA; [c]Department of Gastroenterological Surgery, Okayama University Graduate School of Medicine, Dentistry and Pharmaceutical Sciences, Okayama, Japan; [d]Center for Innovative Clinical Medicine, Okayama University Hospital, Okayama, Japan; [e]Oncolys Biopharma, Inc., Tokyo, Japan

ABSTRACT

We previously demonstrated that quiescent cancer cells in a tumor are resistant to conventional chemotherapy as visualized with a fluorescence ubiquitination cell cycle indicator (FUCCI). We also showed that proliferating cancer cells exist in a tumor only near nascent vessels or on the tumor surface as visualized with FUCCI and green fluorescent protein (GFP)-expressing tumor vessels. In the present study, we show the relationship between cell-cycle phase and chemotherapy-induced tumor angiogenesis using *in vivo* FUCCI real-time imaging of the cell cycle and nestin-driven GFP to detect nascent blood vessels. We observed that chemotherapy-treated tumors, consisting of mostly of quiescent cancer cells after treatment, had much more and deeper tumor vessels than untreated tumors. These newly-vascularized cancer cells regrew rapidly after chemotherapy. In contrast, formerly quiescent cancer cells decoyed to S/G_2 phase by a telomerase-dependent adenovirus did not induce tumor angiogenesis. The present results further demonstrate the importance of the cancer-cell position in the cell cycle in order that chemotherapy be effective and not have the opposite effect of stimulating tumor angiogenesis and progression.

ARTICLE HISTORY
Received 15 July 2016
Accepted 31 July 2016

KEYWORDS
angiogenesis; cell cycle; chemotherapy; decoy; FUCCI; imaging; resistance; quiescence

Introduction

The phase of the cell cycle is the main determinant whether a cancer cell can respond to a given drug. We previously monitored the cell cycle dynamics of cancer cells throughout a live tumor intravitally using a fluorescence ubiquitination cell cycle indicator (FUCCI) and observed that more than 80% of internal cancer cells of an established tumor are quiescent in G_0/G_1 phase. FUCCI imaging demonstrated that cytotoxic agents had little effect on quiescent cancer cells, which are the vast majority of an established tumor. Drug-resistant quiescent cancer cells restarted cycling after the cessation of chemotherapy as they reached the surface of the tumor. These results indicate why most drugs currently in clinical use, which target cancer cells in $S/G_2/M$, are mostly ineffective on solid tumors.[1] We have termed this phenomena tumor intrinsic chemoresistance (TIC).[2] The results also suggest that drugs that target quiescent cancer cells are urgently needed.[1]

In the present study, we demonstrate that dormant/quiescent cancer cells induce nascent tumor vessels after chemotherapy, allowing tumors to regrow rapidly after cessation of treatment. Chemotherapy-treated tumors had much more and deeper tumor vessels than control tumors and rapidly began regrowing after cessation of treatment. This report further suggests that quiescent cancer cells can play a large role in tumor angiogenesis, progression, and drug resistance.

Results and discussion

Quiescent cancer cells within the tumor were resistant to chemotherapy, which further increased the percent of quiescent cells

FUCCI-expressing MKN45 subcutaneous tumors were treated with cisplatinum (CDDP), paclitaxel (PXT), or doxorubicin (DOX) 14 d after implantation. FUCCI-expressing MKN45-derived subcutaneous tumors consisted mostly of quiescent cancer cells, 7 d after 3 cycles of chemotherapy, even increasing their percentage of quiescent cancer cells compared to control. By 21 d after treatment, the tumors had numerous cycling cancer cells at their surface that were formerly quiescent (Fig. 1).[1]

A tumor 7 d after implantation consisted of 15.3 ± 2.4% quiescent cancer cells and 84.7 ± 2.4% proliferating cancer cells. A tumor 14 d after implantation consisted of 52.4 ± 3.5% quiescent cancer cells and 47.6 ± 3.5% proliferating cancer cells. A tumor 21 d after implantation consisted of 67.5 ± 3.5% quiescent cancer cells and 32.5 ± 3.5% proliferating cancer cells (Fig. 2C).[1]

Tumors 3 d after implantation were sensitive to CDDP (Fig. 2A and 2B). In contrast, tumors 14 d after implantation were resistant to chemotherapy (Fig. 2A and 2B). Therefore, we investigated the relationship of the efficacy of

CONTACT Toshiyoshi Fujiwara, M.D., Ph.D. toshi_f@md.okayama-u.ac.jp Department of Gastroenterological Surgery, Okayama University Graduate School of Medicine, Dentistry, and Pharmaceutical Sciences, Okayama, Japan; Robert M. Hoffman all@anticancer.com, AntiCancer, Inc., 7917 Ostrow Street, San Diego, CA, 92111, USA.

Color versions of one or more of the figures in the article can be found online at www.tandfonline.com/kccy.

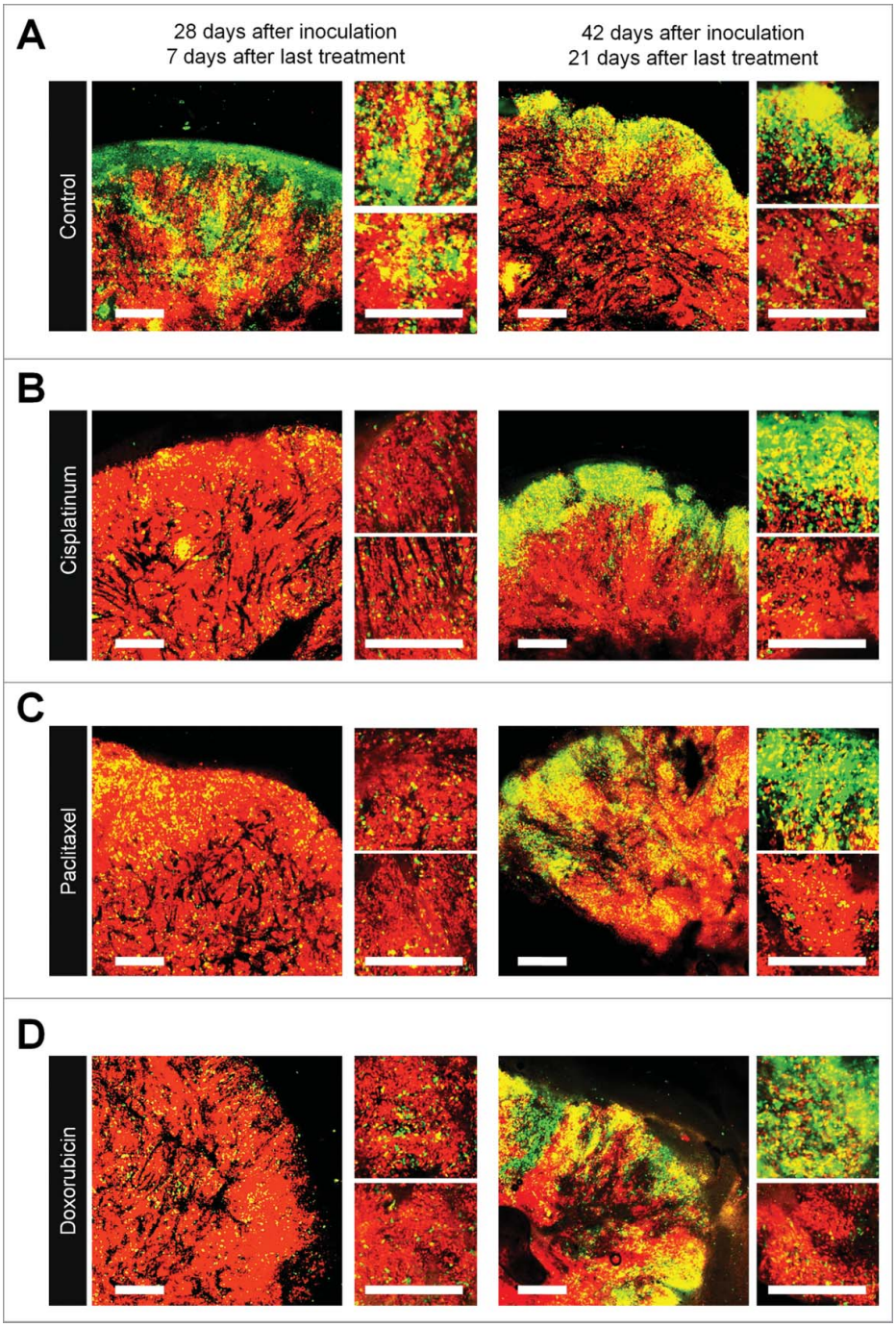

Figure 1. Quiescent cancer cells are resistant to chemotherapy. Experimental setup: FUCCI-expressing MKN45 cells (5×10^6 cells/mouse) were injected subcutaneously into the left flanks of nude mice. When the tumors reached approximately 6 mm in diameter (tumor volume, 80–100 mm^3), mice were intraperitoneally injected with cisplatinum (CDDP) (4 mg/kg), paclitaxel (PTX) (5 mg/kg) or doxorubicin (DOX) (6 mg/kg) for 3 cycles every 3 d. Representative images of cross-sections of FUCCI-expressing MKN45 subcutaneous tumor of control (A), treated with CDDP (B), PTX (C), or DOX (D) 7 d and 21 d after last treatments. Low-magnification image (left). High-magnification image (right). Superficial area image (upper right), deep area image (lower right of the upper and lower subpanels, respectively, in each panel). The cells in G_0/G_1, S, or G_2/M phases appear red, yellow, or green, respectively. (E, F) Histograms show cell-cycle phase of FUCCI-expressing MKN45 subcutaneous tumors of control (A); treated with CDDP (B); PTX (C); or DOX (D). Data are shown as means ± SD (n = 5). Scale bars, 500 μm.

chemotherapy and percentage of quiescent cancer cells in a tumor at the start of chemotherapy: 3 days, 7 days, or 14 d after implantation. The percentage of quiescent cancer cells negatively correlated with the efficacy of chemotherapy (Fig. 2C). Furthermore, the time to recurrence positively correlated with the frequency of quiescent cells (Fig. 2D).

Untreated quiescent cancer cells did not induce tumor angiogenesis

We implanted FUCCI-expressing MKN45 cells in the flank subcutaneously in nestin-GFP transgenic nude mice, where nascent tumor vessels express GFP.[3] Seven days after implantation, nascent tumor vessels reached the center of

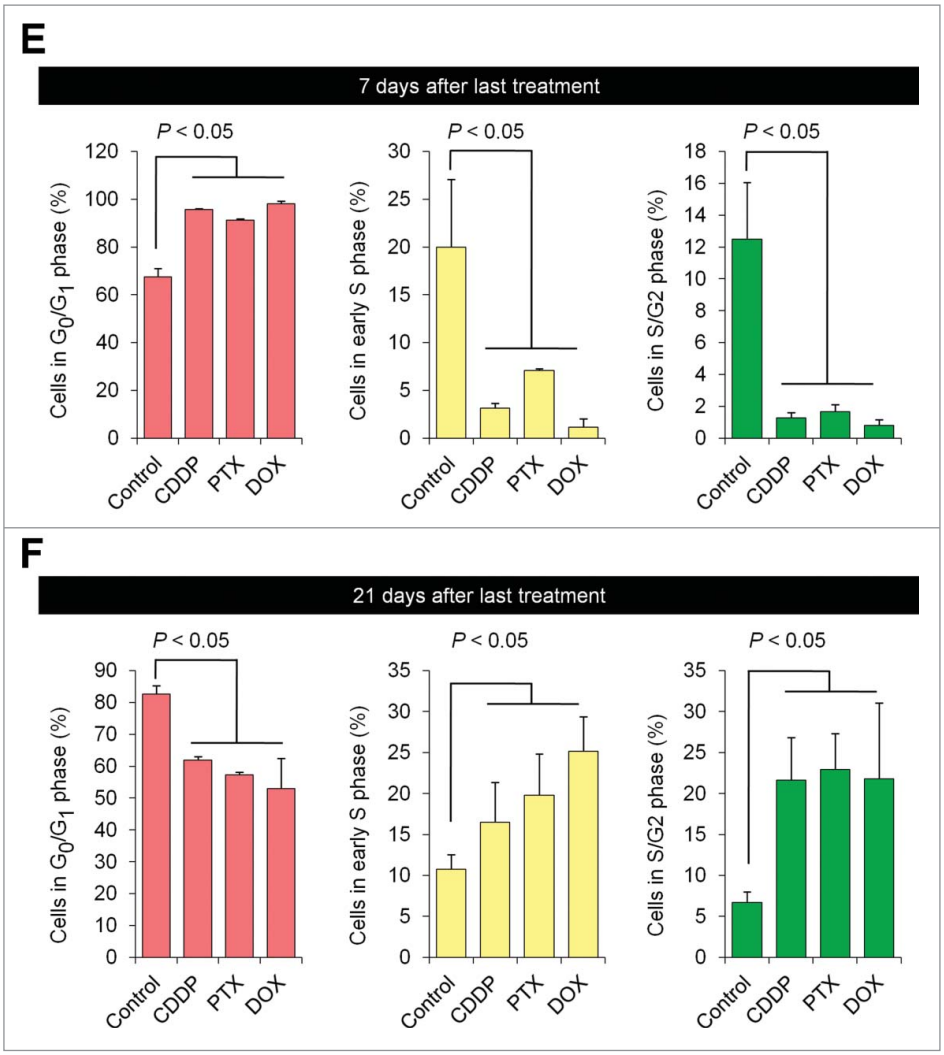

Figure 1. (Continued)

tumors (Fig. 3A). In contrast, 28 d after implantation, nascent tumor vessels reached only the surface area, where proliferating cancer cells were located (Fig. 3A). There were few nascent vessels near quiescent cancer cells (Figs. 3A and 3B).

Chemotherapy-treated quiescent cancer cells induced tumor angiogenesis

FUCCI-expressing tumors were treated with CDDP, PTX, or DOX 14 d after implantation in nestin-GFP transgenic nude mice. Chemotherapy-treated FUCCI-expressing tumors had more nestin-GFP nascent tumor vessels compared with non-treated tumors 7 d after the last treatment of CDDP (Fig. 4B), PTX (Fig. 4C), or DOX (Fig. 4D) compared with control tumor (Fig. 4A). The number of vessels increased after treatment in the deeper areas of the tumors, which contained quiescent cells, but not in the superficial area which contained cycling cells (Fig. 4E). Moreover, nascent tumor vessels in the center area in the chemotherapy-treated tumors were longer than non-treated tumors (Fig. 4F).

Chemotherapy-treated-tumors maintained nascent tumor vessels in their central area when tumors regrew after chemotherapy

Even 21 d after the last treatment, chemotherapy-treated tumors had more nascent vessels compared with non-treated tumors. More proliferating cancer cells were located near the nascent tumor vessels in the chemotherapy-treated tumors than non-treated tumors. These results suggested that conventional chemotherapy induces tumor angiogenesis, resulting in increased tumor aggressiveness.

Decoy therapy reduces tumor angiogenesis

We previously reported viral-induced[4] or bacteria-induced decoy[5] of quiescent cancer cells within the tumor from G_0/G_1 phase to S/G_2 phase, which converts them to chemosensitivity. FUCCI-expressing tumors in ND-GFP transgenic nude mice were first treated with telomerase-dependent adenovirus OBP-301. Decoyed tumors had fewer tumor vessels than non-treated tumors 21 d after the last chemotherapy, as well as 7 d after the last treatment

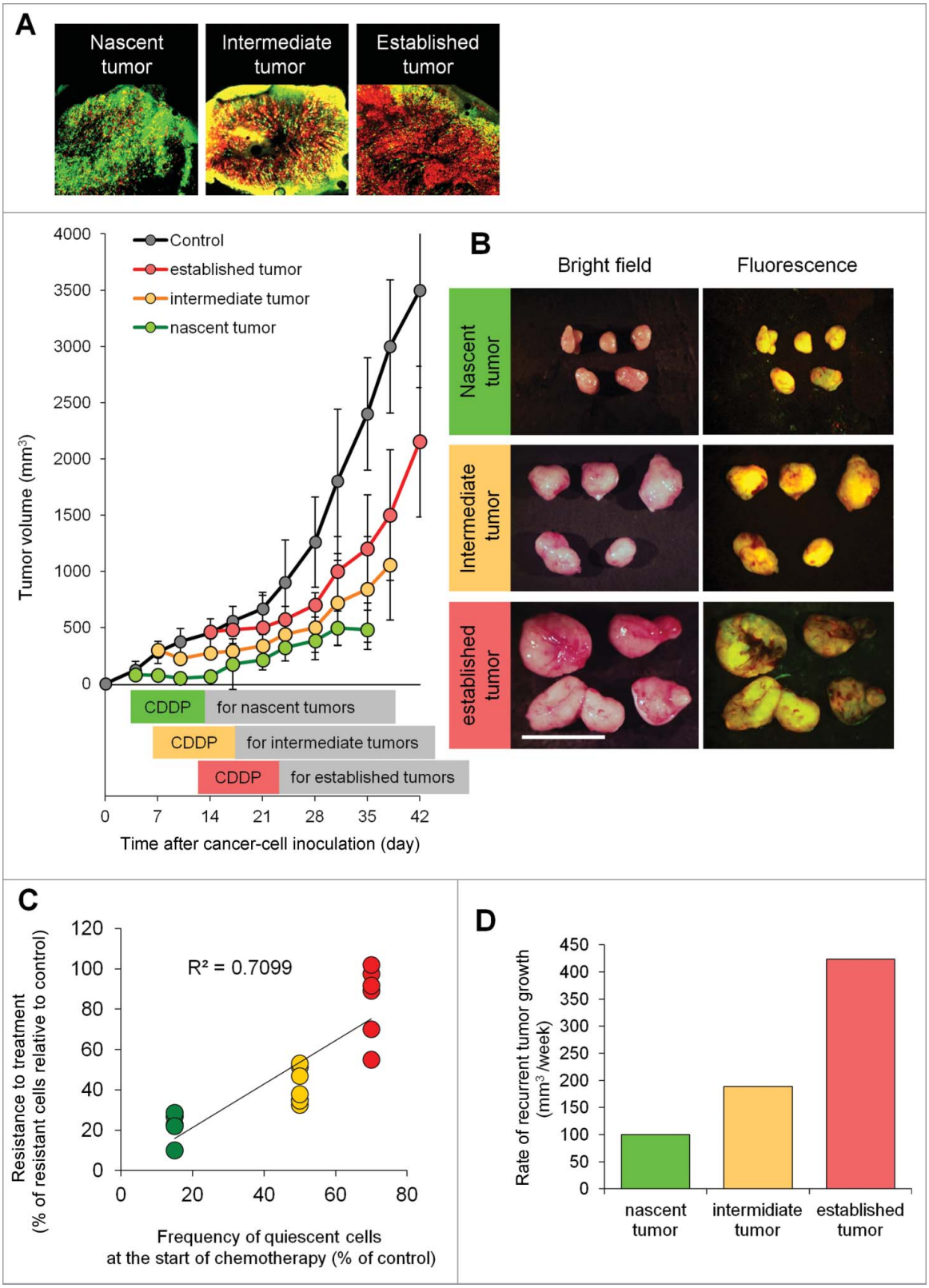

Figure 2. Efficacy of chemotherapy is inversely dependent on the percentage of quiescent/dormant cancer cells. (A) Representative image of cross section of nascent tumor (3 d after cancer cell inoculation), intermediate tumor (7 d after cancer cell inoculation), and established tumor (14 d after cancer cell inoculation). Experimental setup; FUCCI-expressing MKN45 cells (5×10^6 cells/mouse) were injected subcutaneously into the left flanks of mice. Mice were intraperitoneally injected with cisplatinum (CDDP) (4 mg/kg) 3 d after inoculation, 7 d after inoculation, or 14 d after inoculation for 3 cycles every 3 d. (B) Representative images of CDDP-treated FUCCI-expressing MKN45 subcutaneous tumors. Nascent tumor (treatment started 3 d after inoculation) (upper). Intermediate tumor (treatment started 7 d after inoculation) (middle). Established tumor (treatment started 14 d after inoculation) (lower). (C) The relationship between antitumor efficacy of CDDP and the percentage of quiescent cancer cells. (D) Bar graphs show the relationship between rate of recurrent tumor growth and the cell-cycle status of tumors. The cells in G_0/ G_1, S, or G_2/M phases appear red, yellow, or green, respectively. Data are shown as means ± SD (n = 5). Scale bars, 500 μm.

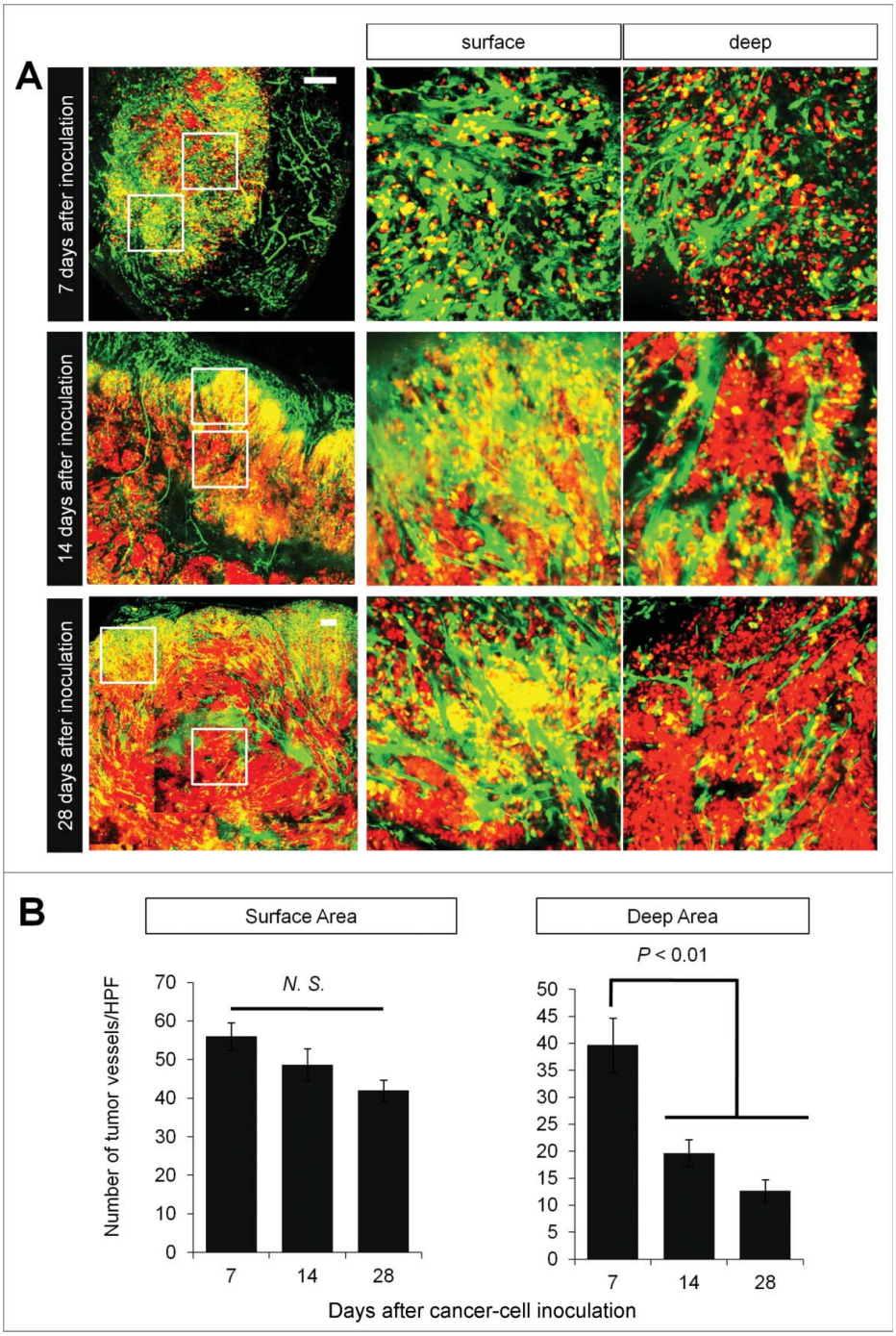

Figure 3. Time-course imaging of FUCCI-expressing tumor in nestin-GFP driven transgenic nude mice. Experimental setup. FUCCI-expressing MKN45 cells (1×10^7 cells/mouse) were injected subcutaneously into the left flanks of nestin-GFP transgenic mice. (A) Representative image of cross section of nascent tumor (7 d after inoculation), intermediate tumor (14 d after inoculation), and established tumor (28 d after inoculation). (B) Bar graphs show the number of nascent tumor vessels/high powerfield (HPF) at different time points after cancer-cell inculation at the surface of deep area of tumors.

(Fig. 5). Decoyed S/G_2 phase cancer cells lost their ability to induce nascent tumor tumor vessels after chemotherapy.

Conclusions

The present report and our previous studies[1,2,4-10] have demonstrated the contribution of quiescent cancer cells to tumor chemoresistance. The present report demonstrates that in addition to being chemoresistant, quiescent cancer cells within tumors induce angiogenesis after chemotherapy. This effect can be overcome by cell-cycle decoy by a tumor-specific adenovirus, further indicating the potential of decoy chemotherapy.[1,2,4,5,10]

Materials and methods

Cells

MKN45 is a radio-resistant poorly-differentiated stomach adenocarcinoma-derived from a liver metastasis of a patient.[11] The cells were grown in RPMI 1640 medium with 10% fetal bovine serum and penicillin/streptomycin.[1]

Establishment of MKN45 cells stably transfected with FUCCI-vector plasmids

For cell-cycle-phase visualization, the FUCCI (fluorescent ubiquitination-based cell-cycle indicator) expression system was used.[12] Plasmids expressing mKO2-hCdt1 (red/orange fluorescent protein) or mAG-hGem (green fluorescent protein) were obtained from the Medical and Biological Laboratory (City, Japan).[1]

Animal experiments

Athymic *nu/nu* nude mice (AntiCancer, Inc.) were bred and maintained in a barrier facility under HEPA filtration and fed with autoclaved laboratory rodent diet (Teklad LM-485; Harlan).[1] Nestin-driven green fluorescent protein (ND-GFP) transgenic nude mice carry the GFP gene under the control of the nestin promoter, were also bred and maintained at AntiCancer

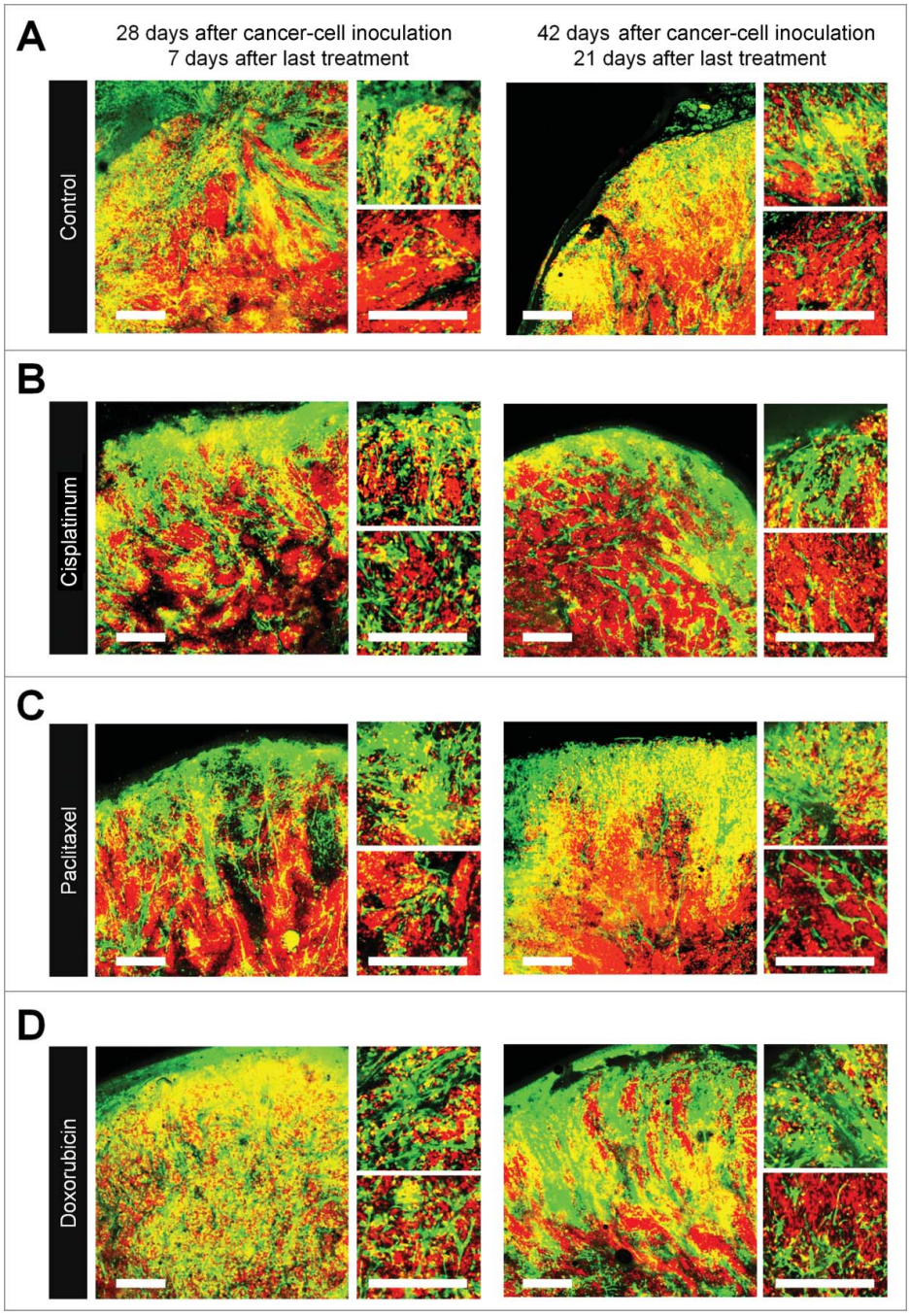

Figure 4. Quiescent/dormant cancer cells induce nascent tumor vessels after chemotherapy. Experimental setup: FUCCI-expressing MKN45 cells (1×10^7 cells/mouse) were injected subcutaneously into the left flanks of nestin-GFP transgenic nude mice. When the tumors reached approximately 6 mm in diameter (tumor volume, 80–100 mm^3), mice were intraperitoneally injected with CDDP (4 mg/kg), PAX (5 mg/kg) or DOX (6 mg/kg) for 3 cycles every 3 d. Representative images of cross-sections of FUCCI-expressing MKN45 subcutaneous tumor of control (A), treated with CDDP (B), PTX (C), or DOX (D) 7 d and 21 d after last treatment. Low-magnification image (left). High-magnification image (right). Superficial area image (upper right). Deep area image (lower right). The cells in G_0/G_1, S, or G_2/M phases appear red, yellow, or green, respectively. (D) Histograms show the number of tumor vessels in the surface area or the center area in tumor of control, CDDP, PAX, or DOX 7 d after last treatment. (E) Bar graphs show the number of tumor vessels at the surface and deep area of control, CDDP-, PAX-, or DOX-treated tumors 21 d after last treatment. (F) Shows length of tumor vessels of control, CDDP-, PAX-, or DOX-treated tumors 21 d after last treatment. Data are shown as means ± SD (n = 5). Scale bars, 500 μm.

Inc.[3,13-15] All animal studies were conducted in accordance with the principles and procedures outlined in the National Institute of Health Guide for the Care and Use of Animals under Assurance Number A3873-1.

Subcutaneous tumor model

All animal procedures were performed under anesthesia using s.c. administration of a ketamine mixture (10 μl ketamine HCl, 7.6 μl xylazine, 2.4 μl acepromazine maleate, and 10 μl PBS) (Henry-Schein, San Diego, CA). FUCCI-expressing MKN454 cells were harvested by brief trypsinization. Single-cell suspensions were prepared at a final concentration of 5×10^6 cells/50 μl. FUCCI-expressing MKN45 cells were inoculated into the flank of nude mice.

FUCCI nestin-driven GFP (ND-GFP) tumor model

FUCCI-expressing MKN45 cells were harvested by brief trypsinization. Single-cell suspensions were prepared at a final concentration of 1×10^7 cells/50 μl. FUCCI-expressing MKN45 cells were implanted into the flank of ND-GFP transgenic nude mice.

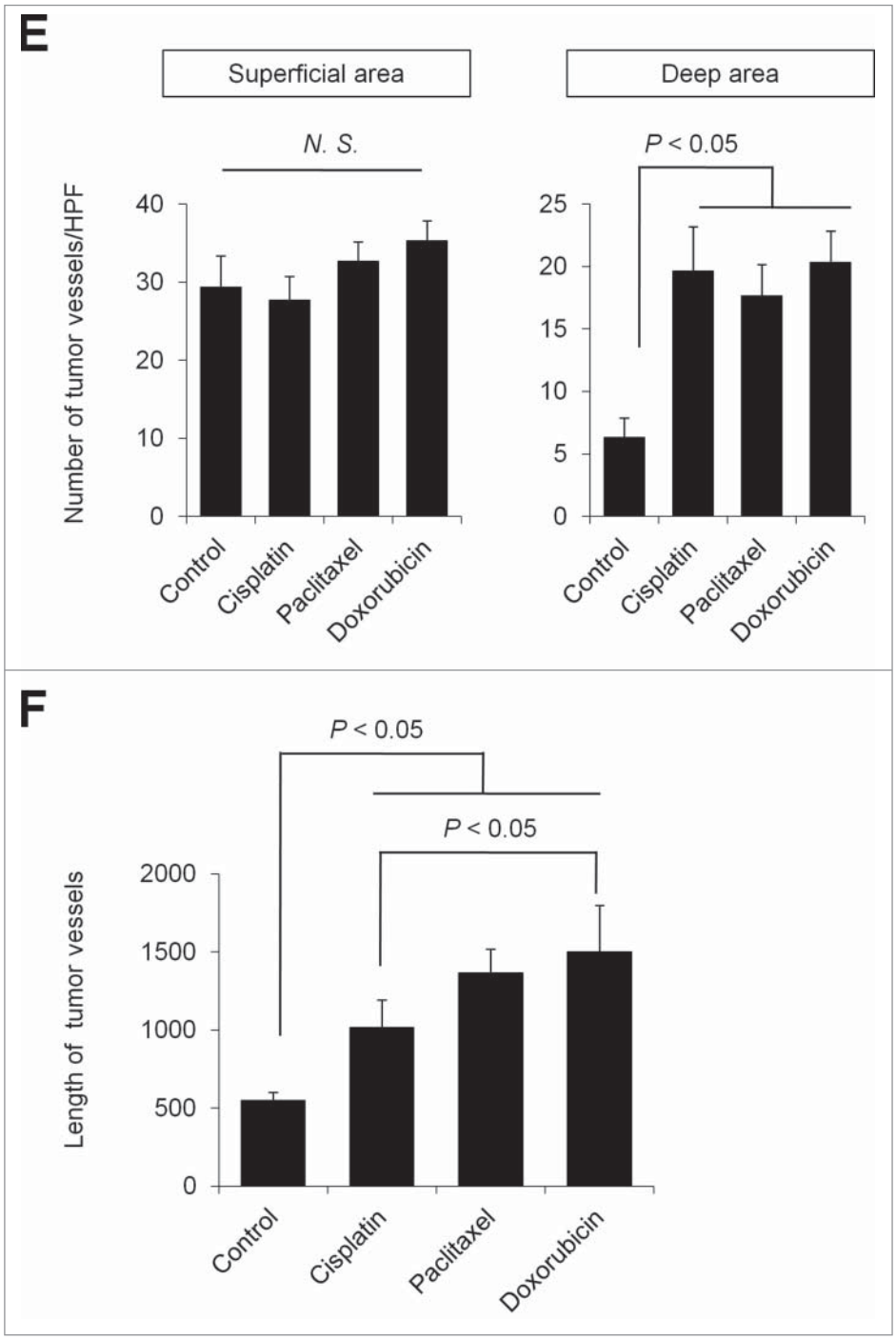

Figure 4. (Continued)

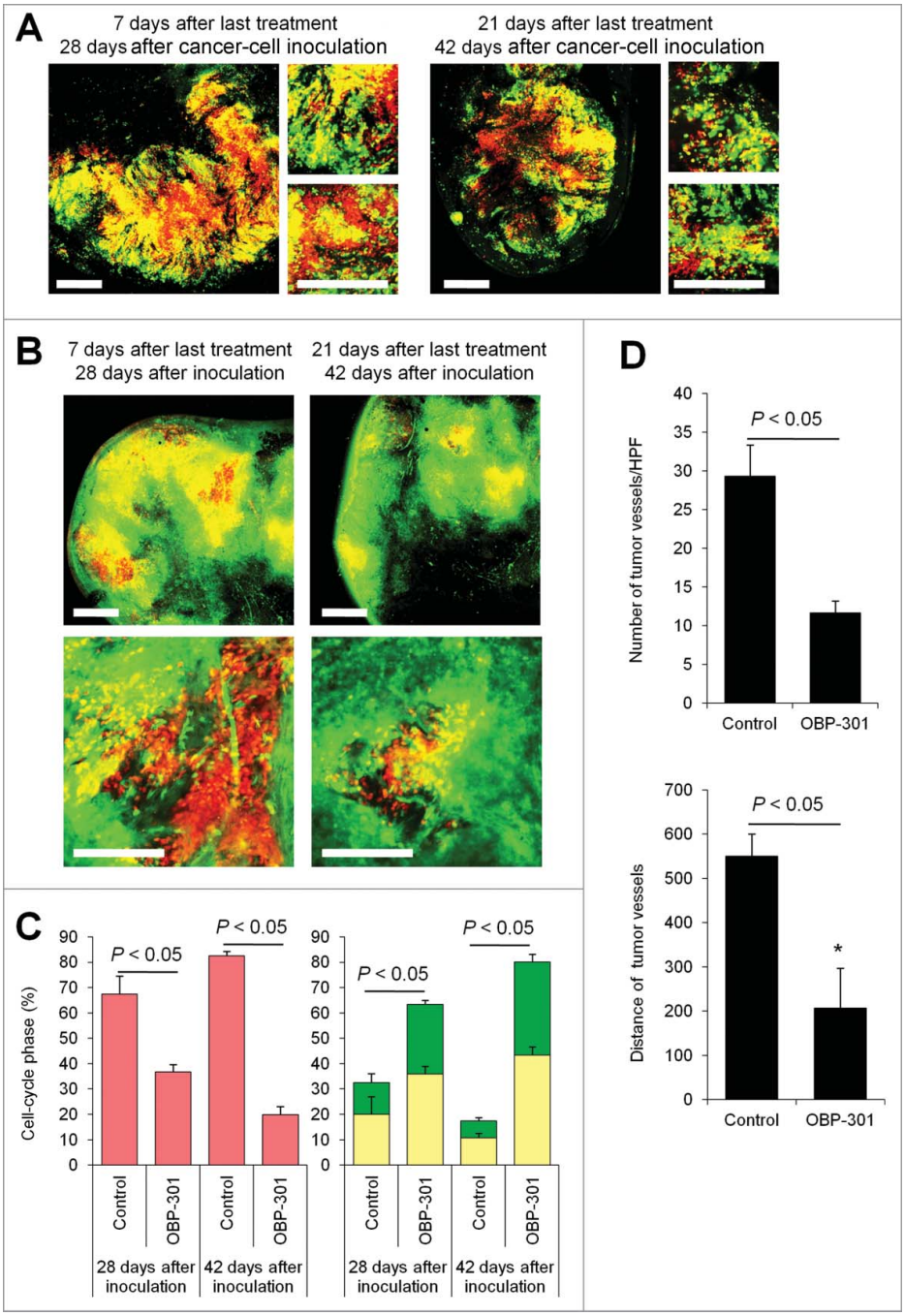

Figure 5. Cell-cycle decoy by telomerase-dependent adenovirus OBP-301 prevents chemotherapy-induced angiogenesis. FUCCI-expressing MKN45 cells (5×10^6 cells/mouse) were injected subcutaneously into the left flanks of nestin-GFP transgenic nude mice. When the tumors reached approximately 6 mm in diameter (tumor volume, 80–100 mm^3), mice were intratumorally injected with OBP-301 for 3 cycles every 3 d. (A, B) Representative images of cross-section of FUCCI-expressing MKN45 subcutaneous tumor treated with OBP-301 in nude mice (A) or nestin-GFP transgenic mice (B). (C) Histograms show cell-cycle phase of FUCCI-expressing MKN45 subcutaneous tumors treated with OBP-301. (D) Bar graphs show the number of tumor vessels in the surface area or the center area in tumor of control or treated with OBP-301 7 d after last treatment. (E) Bar graphs show the distance of tumor vessels from the surface area in control tumor or tumors, treated with OBP-301 21 d after last treatment. Data are shown as means ± SD (n = 5). Scale bars, 500 μm. G_0G_1-phase cancer cells are red; S-phase cancer cells appear yellow; and S/G_2-phase cells appear green in A, B, and represented as such in the histograms of C.

Confocal laser microscopy

Confocal laser scanning microscopy (CLSM) was performed using the FV-1000 (Olympus Corp.) with 2-laser diodes (473 nm and 559 nm). A 4× (0.20 numerical aperture immersion) objective lens and 20 × (0.95 numerical aperture immersion) objective lens (Olympus) were used. Scanning and image acquisition were controlled by Fluoview software (Olympus).[16]

Treatment of nascent, intermediate, or established FUCCI-expressing MKN45 tumors

To evaluate the *in vivo* antitumor efficacy of CDDP against nascent, intermediate, or established tumors, CDPP (4 mg/kg) was injected intraperitoneally into mice with a subcutaneous tumor at 3 d (for nascent tumors), 7 d (for intermediate tumors), or 14 d (established tumors) after implantation. Mice were treated every 3 d for a total of 3 times.

Imaging of angiogenesis after chemotherapy

To evaluate the *in vivo* angiogenesis after chemotherapy, CDDP (4 mg/kg), PAX (5 mg/kg), or DOX (6 mg/kg) were injected intraperitoneally into ND-GFP nude mice with a subcutaneous tumor at 14 d after implantation. Mice were treated every 3 d for a total of 3 times.

Imaging of angiogenesis after infection with adenovirus OBP-301

To evaluate *in vivo* angiogenesis after viral infection, OBP-301 (1×10^8 PFU) was injected into a subcutaneous tumor at 14 d after inoculation. Mice were treated every 3 d for a total of 3 times.

Statistical analysis

Data are shown as means ± SD. For comparison between 2 groups, significant differences were determined using the Student's *t*-test. For comparison of more than 2 groups, statistical significances were determined with a one-way analysis of variance (ANOVA) followed by a Bonferroni multiple group comparison test. *P*-values of < 0.05 were considered significant.

Disclosure of potential conflicts of interest

S. Yano, K. Takehara, and R.M. Hoffman are unsalaried associates of AntiCancer, Inc. H. Tazawa and T. Fujiwara are consultants to Oncolys biopharma, Inc. Y Urata is CEO of Oncolys Biopharma, Inc.

Funding

This study was supported in part by grants from the Ministry of Health, Labor, and Welfare, Japan (to T. Fujiwara; No. 10103827, No. 13801426, No. 14525167) and grants from the Ministry of Education, Culture, Sports, Science and Technology, Japan (to T. Fujiwara; No. 25293283).

Dedication

This paper is dedicated to the memory of A.R. Moossa, MD, and Sun Lee, MD.

References

[1] Yano S, Zhang Y, Miwa S, Tome Y, Hiroshima Y, Uehara F, Yamamoto M, Suetsugu A, Kishimoto H, Tazawa H, et al. Spatial-temporal FUCCI imaging of each cell in a tumor demonstrates locational dependence of cell cycle dynamics and chemoresponsiveness. Cell Cycle 2014; 13:2110-9; PMID:24811200; http://dx.doi.org/10.4161/cc.29156

[2] Yano S, Takehara K, Zhao M, Tan Y, Han Q, Li S, Bouvet M, Fujiwara T, Hoffman RM. Tumor-specific cell-cycle decoy by *Salmonella typhimurium* A1-R combined with tumor-selective cell-cycle trap by methioninase overcome tumor intrinsic chemoresistance as visualized by FUCCI imaging. Cell Cycle 2016; 15:1715-23.

[3] Amoh Y, Li L, Yang M, Moossa AR, Katsuoka K, Penman S, Hoffman RM. Nascent blood vessels in the skin arise from nestin-expressing hair follicle cells. Proc Natl Acad Sci USA 2004; 101:13291-5; PMID:15331785; http://dx.doi.org/10.1073/pnas.0405250101

[4] Yano S, Tazawa H, Hashimoto Y, Shirakawa Y, Kuroda S, Nishizaki M, Kishimoto H, Uno F, Nagasaka T, Urata Y, et al. A genetically engineered oncolytic adenovirus decoys and lethally traps quiescent cancer stem-like cells into $S/G_2/M$ phases. Clin Cancer Res 2013; 19:6495-505; PMID:24081978; http://dx.doi.org/10.1158/1078-0432.CCR-13-0742

[5] Yano S, Zhang Y, Zhao M, Hiroshima Y, Miwa S, Uehara F, Kishimoto H, Tazawa H, Bouvet M, Fujiwara T, Hoffman RM. Tumor-targeting *Salmonella typhimurium* A1-R decoys quiescent cancer cells to cycle as visualized by FUCCI imaging and become sensitive to chemotherapy. Cell Cycle 2014; 13:3958-63; PMID:25483077; http://dx.doi.org/10.4161/15384101.2014.964115

[6] Yano S, Miwa S, Mii S, Hiroshima Y, Uehara F, Yamamoto M, Kishimoto H, Tazawa H, Bouvet M, Fujiwara T, Hoffman RM. Invading cancer cells are predominantly in G_0/G_1 resulting in chemoresistance demonstrated by real-time FUCCI imaging. Cell Cycle 2014; 13:953-60; PMID:24552821; http://dx.doi.org/10.4161/cc.27818

[7] Yano S, Li S, Han Q, Tan Y, Bouvet M, Fujiwara T, Hoffman RM. Selective methioninase-induced trap of cancer cells in S/G_2 phase visualized by FUCCI imaging confers chemosensitivity. Oncotarget 2014; 5:8729-36; PMID:25238266; http://dx.doi.org/10.18632/oncotarget.2369

[8] Yano S, Miwa S, Mii S, Hiroshima Y, Uehara F, Kishimoto H, Tazawa H, Zhao M, Bouvet M, Fujiwara T, Hoffman RM. Cancer cells mimic *in vivo* spatial-temporal cell-cycle phase distribution and chemosensitivity in 3-dimensional Gelfoam® histoculture but not 2-dimensional culture as visualized with real-time FUCCI imaging. Cell Cycle 2015; 14:808-19; PMID:25564963; http://dx.doi.org/10.1080/15384101.2014.1000685

[9] Yano S, Takehara K, Tazawa H, Kishimoto H, Urata Y, Kagawa S, Fujiwara T, Hoffman RM. Therapeutic efficacy in vivo of a telomerase-dependent adenovirus in an orthotopic model of chemotherapy-resistant human stomach carcinomatosis peritonitis visualized with cell cycle color coding FUCCI imaging. J Cell Biochem 2016, Epub ahead of print; http://dx.doi.org/10.1002/jcb.25593

[10] Hoffman RM, Yano S. *Salmonella typhimurium* A1-R and cell-cycle decoy therapy of cancer. Chap. 14. In: Bacterial Therapy of Cancer: Methods and Protocols. Hoffman RM., ed. Methods in Molecular Biology 1409, pp. 165-175. Walker, John M., series ed. Humana Press (Springer Science+Business Media New York), 2016

[11] Yokozaki H. Molecular characteristics of eight gastric cancer cell lines established in Japan. Pathol Int 2000; 50:767-77; PMID:11107048; http://dx.doi.org/10.1046/j.1440-1827.2000.01117.x

[12] Sakaue-Sawano A, Kurokawa H, Morimura T, Hanyu A, Hama H, Osawa H, Kashiwagi S, Fukami K, Miyata T, Miyoshi H, et al. Visualizing spatiotemporal dynamics of multicellular cell cycle progression. Cell 2008; 132:487-98; PMID:18267078; http://dx.doi.org/10.1016/j.cell.2007.12.033

[13] Li L, Mignone J, Yang M, Matic M, Penman S, Enikolopov G, Hoffman RM. Nestin expression in hair follicle sheath progenitor cells. Proc Natl Acad Sci USA 2003; 100:9958-61; PMID:12904579; http://dx.doi.org/10.1073/pnas.1733025100

[14] Amoh Y, Yang M, Li L, Reynoso J, Bouvet M, Moossa AR, Katsuoka K, Hoffman RM. Nestin-linked green fluorescent protein transgenic nude mouse for imaging human tumor angiogenesis. Cancer Res 2005; 65:5352-7; PMID:15958583; http://dx.doi.org/10.1158/0008-5472.CAN-05-0821

[15] Mignone JL, Kukekov V, Chiang AS, Steindler D, Enikolopov G. Neural stem and progenitor cells in nestin-GFP transgenic mice. J Comp Neurol 2004; 469:311-24; PMID:14730584; http://dx.doi.org/10.1002/cne.10964

[16] Uchugonova A, Duong J, Zhang N, König K, Hoffman RM. The bulge area is the origin of nestin-expressing pluripotent stem cells of the hair follicle. J Cell Biochem 2011; 112:2046-50; PMID:21465525; http://dx.doi.org/10.1002/jcb.23122